# Electron cyclotron mass in undoped CdTe/CdMnTe quantum wells

A. A. Dremin,[1,2] D. R. Yakovlev,[1,3] A. A. Sirenko,[4] S. I. Gubarev,[2] O. P. Shabelsky,[2] A. Waag,[5] and M. Bayer[1]
[1]*Experimentelle Physik II, University of Dortmund, D-44227 Dortmund, Germany*
[2]*Institute of Solid State Physics, Chernogolovka, Moscow District, 142432, Russia*
[3]*A.F.Ioffe Physico-Technical Institute, Russian Academy of Sciences, 194021 St. Petersburg, Russia*
[4]*New Jersey Institute of Technology, Newark, New Jersey 07102, USA*
[5]*Institute of Semiconductor Technology, Braunschweig Technical University, 38106 Braunschweig, Germany*
(Received 19 January 2005; revised manuscript received 15 August 2005; published 23 November 2005)

Optically detected cyclotron resonance of two-dimensional electrons has been studied in nominally undoped CdTe/(Cd,Mn)Te quantum wells. The enhancement of carrier quantum confinement results in an increase of the electron cyclotron mass from $0.099m_0$ to $0.112m_0$ with well width decreasing from 30 down to 3.6 nm. Comparison with model calculations performed for this material system highlights two contributions to the mass increase, the first one determined by band structure parameters and the second one due to the polaron effect modified by reducing the dimensionality of the electronic system.

DOI: 10.1103/PhysRevB.72.195337 PACS number(s): 73.21.Fg, 76.40.+b, 71.35.Pq, 78.55.Et

## I. INTRODUCTION

The effective masses of carriers (electrons and holes) are among the basic parameters for semiconductors and semiconductor heterostructures. Nowadays exhaustive information is available for heterostructures based on III-V semiconductors—e.g., GaAs/(Al,Ga)As heterosystems. However, only limited experimental data have been reported so far for the II-VI family of semiconductor heterostructures. Among them are the structures based on CdTe, which are rather popular for optical studies. One of the attractions of this material is the possibility to introduce magnetic Mn ions in the cation sublattice. The strong exchange interaction of free carriers with localized spins of magnetic ions gives rise to giant magneto-optical effects—e.g., the giant Zeeman splitting of the band states, giant Faraday rotation, etc.[1] (Cd,Mn)Te, (Cd,Mg)Te, and (Cd,Zn)Te are among the barrier materials to confine carriers in CdTe quantum wells. In this paper we study experimentally the dependence of the electron effective mass on quantum well (QW) width for CdTe/(Cd,Mn)Te heterostructures.

The cyclotron resonance (CR) technique is widely used for evaluation of the fundamental parameters of heterostructures, including the carriers effective masses. It has been recently applied to modulation-doped CdTe/(Cd,Mg)Te QW's, and the electron effective mass has been measured for these QW's with widths varied between 7.5 and 30 nm (Refs. 2 and 3) each, with a two-dimensional (2D) electron gas density of $4\times10^{11}$ cm$^{-2}$. One of the impediments for the conventional cyclotron resonance technique is that the carrier density has to be large enough to produce a noticeable change in the absorption of microwave or far-infrared (FIR) radiation. This limitation does not allow us to measure carrier effective masses in undoped systems. It has been overcome by the invention of the optically detected cyclotron resonance (ODCR or ODR) technique (see Ref. 4 and references therein).

The ODR technique is based on variation of the optical properties, such as the photoluminescence intensity under absorption of microwaves or FIR radiation by free carriers. It has proved to be extremely sensitive and has been successfully used to measure the effective masses of electrons and holes in bulk GaAs, InP, CdTe,[5–7] and SiC.[8] It was also developed to study 2D electron states in GaAs/(Al,Ga)As heterostructures[9–11] and internal transitions of neutral and charged magnetoexcitons.[12–14] Another advantage of the ODR technique is related to its spectral selectivity, which allows for selecting the signal from different quantum wells grown in the same structure by analyzing the corresponding photoluminescence emission lines. Therefore, the ODR technique is very well suited for measurements of the electron effective masses in undoped CdTe-based QW's of different widths.

## II. EXPERIMENT

We have studied a CdTe/$Cd_{0.86}Mn_{0.14}Te$ quantum heterostructure grown by molecular beam epitaxy on an (100)-oriented CdTe substrate. The structure contains four consequently grown CdTe wells with width $L_Z$=30, 9, 3.6, and 1.2 nm separated by 50-nm-thick $Cd_{0.86}Mn_{0.14}Te$ barriers from each other. The samples were nominally undoped, but a residual *n*-type doping of the barrier layers provides free electrons in CdTe quantum wells. The concentration of these electrons evaluated from the optical spectra does not exceed $5-8\times10^9$ cm$^{-2}$. The presence of these electrons results in observation of the charged exciton complexes in the emission spectra. Typical photoluminescence (PL) and reflectivity spectra of such structures can be found in Refs. 15–17.

Experiments were carried out at a temperature of $T$=4.2 K in a He exchange cryostat in magnetic fields up to $B$=8.3 T. The sample was mounted on a rotating platform, which enables ODR measurements in tilted magnetic fields in order to check the two-dimensional character of the studied resonances. Most experimental data were collected in magnetic fields oriented parallel to the structure growth axis ($\theta=0°$) with the cyclotron motion of electrons in the plane of the quantum wells. Photoexcitation of the samples by a HeNe laser and collection of the luminescence signal were provided via optical fibers. The spot of the HeNe laser beam ($\lambda$=632.8 nm, power up to 20 mW) was overlapped by the

 

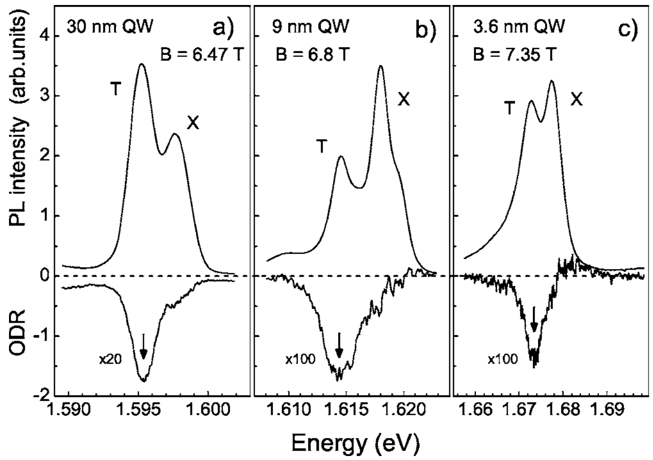


FIG. 1. Photoluminescence and ODR signal spectra measured for CdTe/$Cd_{0.86}Mn_{0.14}$Te QW's with widths equal to (a) 30 nm, (b) 9 nm, and (c) 3.6 nm. Spectra are measured at magnetic fields for which the FIR radiation induces the maximal changes—i.e., under conditions of cyclotron resonance for electrons. $T=4.2$ K. The photon energies corresponding to the maximum of the ODR signal are marked with arrows. Note that the magnetic field scans of the cyclotron resonances shown in Fig. 3 were detected at these energies.

spot of a $CO_2$ pumped FIR laser with the radiation wavelength of $\lambda_{FIR}=163$ $\mu$m ($E_{FIR}=7.6$ meV) and cw power up to 15 mW. FIR radiation was guided into the cryostat via a stainless steel pipe and focused on the sample by a Teflon lens. The photoluminescence signal was analyzed with a 0.6-m single-grating spectrometer equipped with a cooled photomultiplier.

The FIR laser beam was mechanically chopped. The influence of the FIR radiation on the PL spectra was synchronously detected by a lock-in amplifier at various magnetic fields. The ODR signal was normalized to the PL intensity $I(B)$ measured at the same wavelength. This procedure allowed us to correct the shape of the resonance profile by accounting for the PL intensity variations with increasing magnetic field.

## III. RESULTS AND DISCUSSION

Photoluminescence spectra for three CdTe/$Cd_{0.86}Mn_{0.14}$Te QW's are shown in Fig. 1. The emission spectra of all three QW's consist of two strong lines corresponding to excitons ($X$) localized at well-width fluctuations and to charged exciton complexes—i.e., trions ($T$)—consisting of two electrons and one hole.[18] Their formation requires an excess of electrons over holes in QW's. Such an excess is typical for unintentionally doped CdTe QW's, due to carrier diffusion from the barrier materials with residual $n$-type doping. The energy difference between the exciton and trion lines varies from 2.5 to 5 meV and increases in narrow wells. It corresponds to the trion binding energy, which is about an order of magnitude smaller than the binding energy of the quasi-2D excitons.

One can also see in Fig. 1 that the exciton emission line shifts from 1.597 up to 1.678 eV for QW width varied from 30 down to 3.6 nm due to the carrier quantum confinement. We use the energy position of the exciton emission to evaluate the QW width for the studied samples. Model calculations for the exciton PL transition energy and the exciton binding energy have been performed using the procedure described in Ref. 19 with the following parameters for our material system: the band-gap offset between the well and barrier materials is 223 meV; it is divided in a ratio of 70/30 between the conduction and valence bands; the dielectric constant $\varepsilon=10$; the in-plane heavy-hole mass was taken as $m_{hh,\parallel}=0.37m_0$; the heavy-hole mass along the growth axis—i.e., perpendicular to the QW plane—is $m_{hh,\perp}=0.48m_0$. We have taken into account eight confined electron levels and ten confined hole levels. The results of our calculations are presented in Fig. 2, from which the widths of the quantum wells have been deduced by comparing the experimental exciton PL transition energies with the calculated dependence.

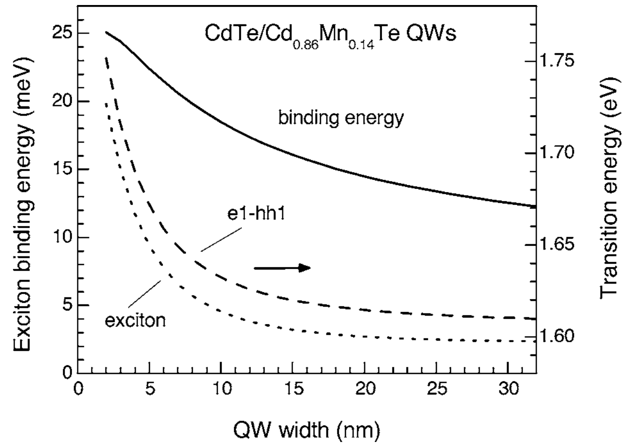


FIG. 2. Exciton energy, exciton binding energy, and energy of the optical transition between the lowest levels of confined electrons and holes ($e$1-hh1) calculated for CdTe/$Cd_{0.86}Mn_{0.14}$Te QW's as a function of the QW width.

We turn now from the sample characterization to the results of the optically detected resonance. ODR signal could be reliably detected in the QW's with widths $L_Z=30$, 9, and 3.6 nm. We have found no influence of FIR radiation on the emission from the narrowest QW with $L_Z=1.2$ nm. Most probably the changes are below the sensitivity level of our setup.

The ODR signal intensity plotted as a function of magnetic field clearly demonstrates a resonance behavior (Fig. 3). We have checked that both the resonance field and the shape of the resonance profile are insensitive to the PL detection energy. The ODR signal was recorded at fixed detection energies shown by the arrows in Fig. 1. The ODR signal was normalized to the PL intensity measured at the same detection energy. For all QW's the PL intensity was decreasing by about 30% with increasing magnetic field from 5.5 T to 8 T. This change has a very small influence on the shape of the resonance profile and requires correction of the resonance field by less than 0.01 T.

There are three characteristics of the resonance curves to be analyzed: (i) the resonance magnetic field $B_R$, which is directly linked to the value of the electron effective mass; (ii)

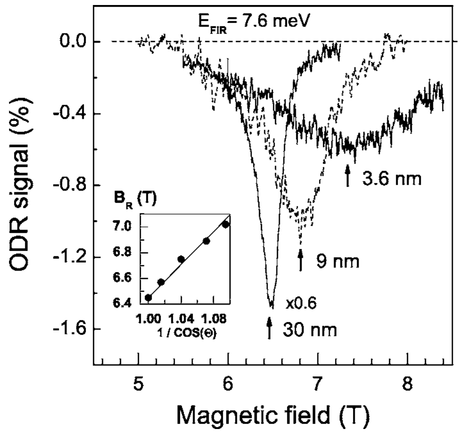


FIG. 3. Magnetic field dependence of ODR signal (in % of PL signal) at $E_{FIR}$=7.6 meV measured in $CdTe/Cd_{0.86}Mn_{0.14}Te$ QW's. The shift of the resonance field is given in the inset as a function of the tilt angle $\theta$ for the 30-nm-wide QW [circles, experiment values; line, fit with $6.45/\cos(\theta)$].

the resonance full width at the half maximum (FWHM), which is inversely proportional to the electron scattering rate and contains information on the electron mobility; and (iii) the resonance amplitude, which is controlled by the mechanisms responsible for the ODR signal. Before proceeding with discussion of the resonance parameters we shall prove that the observed features originate from the QW's. In order to check the two-dimensional character of electrons responsible for the ODR signal we have carried out the same measurements in tilted magnetic fields. The pronounced shift of the CR resonance toward higher magnetic fields was found to be proportional to $1/\cos\theta$ where $\theta$ (being varied from 0° to 24°) is the angle between the magnetic field direction and the structure growth axis. The inset in Fig. 3 illustrates this observation for the 30-nm QW, proving that the electrons have quantum-confined character.

In the widest QW with 30 nm width, the resonance FWHM is 0.33 T. This corresponds to a momentum relaxation time of 2.4 ps and to an electron mobility of $3.0\times10^4$ cm$^2$/(V s). A decrease of the well width is accompanied by a strong broadening of the resonances up to 0.74 T and 1.9 T for 9-nm and 3.6-nm wells, respectively. The corresponding electron mobilities are $1.4\times10^4$ and $0.5\times10^4$ cm$^2$/(V s). Localization of electrons on QW width fluctuations is known to be the dominating mechanism for resonance broadening in low-dimensional structures. Its contribution increases in narrow QW's, causing the decrease of the carrier mobility. The decrease of the electron mobility correlates well with the increasing width of the photoluminescence emission spectra from 1.7 meV to 3.7 meV for 30-nm and 3.6-nm wells, respectively (see Fig. 1).

The modulation spectra (ODR signal) recorded at the resonance magnetic field are shown in the lower panels of Fig. 1. In the 30-nm QW the FIR radiation results in a decrease of the PL signal by approximately 2.5% for the trion line and a significantly smaller decrease for the exciton line. The ODR signal decreases in narrower QW's; it is about 0.9% for the 9-nm QW and only 0.5% for the 3.6-nm QW. This observation can be attributed to enhanced electron localization and the related decrease of the electron mobility in narrow QW's.

The dominating mechanism of the PL intensity modulation under FIR radiation is related to the specifics of the trion complexes in the studied structures. As one can see in Fig. 1, the strongest ODR signal has been observed in the maximum of the trion emission line and only weak modulations are seen for the exciton line. This is expected since in QW's with a very diluted electron gas the trion emission is much more sensitive to the temperature of the electron gas[18,20] than the exciton emission. This is due to the fact that for trion formation one of the electrons is captured from the electron gas and, hence, the probability of trion formation is very sensitive to the electron gas temperature. Heating of the electrons under cyclotron resonance conditions decreases the probability for trion formation, which causes a decrease of the trion emission intensity. We note here that contrary to the behavior in CdTe/(Cd,Mg)Te QW's reported in Refs. 18 and 20 in our samples the decrease of the trion emission does not lead to the respective increase of the exciton emission (see Fig. 1). Most probably nonradiative channels, which are known to be more efficient in (Cd,Mn)Te samples compared with (Cd,Mg)Te ones, are responsible for these appearances.

Measurement of the resonance magnetic field $B_R$, where the FIR energy coincides with the cyclotron energy of electrons, allows evaluation of the electron effective mass. Fitting the resonances shown in Fig. 3 by a Lorenzian function we obtained $B_R$=6.45, 6.75, and 7.25 T for QW's with $L_Z$=30, 9, and 3.6 nm, respectively. The electron cyclotron mass $m_e$ was evaluated from $B_R$ values using $m_e/m_0 = 0.0152 B_R$ [T], which is derived from $m_e = e\hbar B_R/E_{FIR}$ for $E_{FIR}$=7.6 meV. We found that $m_e$ increases with decreasing well width: $m_e=0.099m_0$, $0.104m_0$, and $0.112m_0$ for $L_Z$=30, 9, and 3.6 nm. These data are shown by solid circles in Fig. 4. The arrow in the figure marks the electron effective mass of $0.096m_0$ measured for bulk CdTe.[21] The open circles are experimental data for CdTe/(Cd,Mg)Te QW's with nonmagnetic barriers taken from Ref. 2. These results coincide well with our experimental data. For the studied relatively wide QW's the dominating part of the electron wave function is concentrated in the CdTe wells and is not much dependent on the differences in barrier materials. Also, the (Cd,Mn)Te and (Cd,Mg)Te alloys are pretty similar in their properties as these barrier materials provide efficient confinement of both electrons and holes. One may expect that in doped CdTe/(Cd,Mg)Te QW's $m_e$ will be larger due to nonparabolicity of the conduction band at finite $k$ values given by the Fermi level. However, an estimation of this effect for the electron density of $4\times10^{11}$ cm$^{-2}$ gives an $m_e$ increase by 1.2% only,[2] which does not exceed the error bar for our experimental data. Comparing the data for the two systems with different barrier materials we can conclude that the electron confinement and the respective increase of the quantum confinement energy is the dominating factor in the $m_e$ dependence on the QW width.

For deeper insight into the electron mass behavior we have compared the experimental data with results of model calculations. The electron effective mass in bulk CdTe measured experimentally has a value of $m_e=0.096m_0$.[22–24] This value has a polaron contribution which originates from the

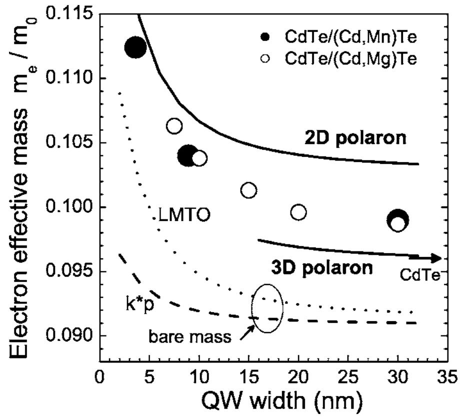


FIG. 4. Electron cyclotron mass versus QW width for CdTe-based quantum wells. Experimental data of this work for $CdTe/Cd_{0.86}Mn_{0.14}Te$ QW's are given by the solid circles. Experimental error bars are smaller than the symbol size. Open circles show the data for the modulation-doped $CdTe/Cd_{0.88}Mg_{0.12}Te$ QW's with electron density of $4\times10^{11}$ $cm^{-22}$. The bare electron mass calculated without polaron correction in a parabolic-band approximation is shown by the dashed line and that with accounting for conduction-band nonparabolicity is given by the dotted line. The solid lines show the linear muffin-tin-orbital (LMTO) calculations with account for 2D and 3D polaron corrections.

cloud of optical phonons that "accompany" the electron and makes the measured mass "heavier."

Results of model calculations provide the so-called "bare" electron effective mass $m_b$ that can be related to the experimentally determined value of the electron mass $m_e$ using the correction for the polaron effect. In bulk materials (i.e., in 3D system),

$$m_e = m_b(1 + \alpha/6), \tag{1}$$

where $\alpha$ is a constant of the electron-phonon interaction, known as a Fröhlich coupling constant. Its calculated value for CdTe of 0.28 (Ref. 25) is in a very good agreement with the experimentally measured one of 0.286 (Ref. 26). With these values one can get $m_b$=0.0916$m_0$ which we will use for the calculations.

A simple analytical approach to calculation of the electron effective mass is provided in the frame of the three-band $\mathbf{k}\cdot\mathbf{p}$ technique,

$$\frac{m_0}{m_b} = (1 + 2F) + \frac{E_P(E_g + 2\Delta_{SO}/3)}{E_g(E_g + \Delta_{SO})}, \tag{2}$$

where $E_P$=21.0 eV is the interband matrix element, $\Delta_{SO}$ =0.93 eV is the spin-orbit splitting, $E_g$=1.59 eV is the fundamental band gap of CdTe, and $F$=−0.83 is a parameter accounting for the contribution of high-energy bands.[27–29]

One can see from Eq. (2) that the effective mass $m_b$ increases for larger band-gap values. Exact calculation of $m_b$ in QW structures requires laborious numerical procedures, which include the quantum confinement energy, conduction-band nonparabolicity, and penetration of the electron wave function into barriers (see, e.g., Refs. 30 and 31). However, the three-band $\mathbf{k}\cdot\mathbf{p}$ approach gives fairly well suited values when $E_g$ in Eq. (2) is replaced by the energy separation between the lowest electron and hole subbands. In Fig. 4 these calculations for CdTe-based QW's in the parabolic band approximation are shown by the dashed line. In order to take into account the conduction-band nonparabolicity in CdTe, we performed more elaborate calculations based on density functional theory in the local density approximation using the LMTO approach.[32] The calculated dependence for the bare electron mass (the dotted line in Fig. 4) demonstrates the main experimental trend of increasing mass values with narrowing QW width.

In order to compare the experimental data with calculations the polaron effect should be taken into account. However, this task is not trivial as the value of the polaron correction to the electron effective mass differs in 3D and 2D systems. In the 3D system it is described by Eq. (1) and in the 2D system it has the following form:

$$m_e = m_b(1 + \pi\alpha/8). \tag{3}$$

In the studied quantum wells electrons have quasi-two-dimensional character and their behavior varies from 3D like in wide QW's towards 2D like in narrow QW's. The transition between these limiting cases is expected to be smooth and monotonic,[2] but the respective calculations are still missing. Therefore, we plot in Fig. 4 two dependences made with 3D and 2D polaron corrections to the LMTO-calculated dependence of $m_b$. It is assumed here that $\alpha$ does not depend on the system dimension, which is in agreement with results reported for CdTe/(Cd,Mn)Te QW's (see Ref. 33 and references therein). It is clearly seen in Fig. 4 that the experimental data fall, as expected, in the range between two calculated limits. Experimental points tends from the 2D limit in narrow QW's to the 3D limit in wide QW's. Therefore, we conclude that the increase of the electron effective mass in narrow QW's predicted by the band structure calculation is additionally increased by the modification of the electron-phonon interaction.

To conclude, the optically detected resonance technique has been used to study electron cyclotron resonance in nominally undoped CdTe/(Cd,Mn)Te QW's. Pronounced modulation of the luminescence intensity has been found for the charged exciton emission when the residual electrons are resonantly heated by FIR radiation. The evaluated electron effective masses increase with narrowing quantum well width and are in good agreement with data for CdTe QW's confined by (Cd,Mg)Te barriers. Comparison with model calculations allows us to conclude about two contributions to the mass increase. The first one is determined by band structure parameters and the second one is due to the polaron effect modified by reducing the dimensionality of the electronic system.

## ACKNOWLEDGMENTS

The authors are grateful to G.V. Astakhov who provided the model calculations for Fig. 2. This work was supported by the QuIST program of DARPA, the "Forschugsband Mikro- und Nanostrukturen" of the University of Dortmund, the BmBF project "nanoquit," and the Russian Foundation for Basic Research.

[1] J. K. Furdyna, J. Appl. Phys. **64**, R29 (1988).
[2] G. Karczewski, T. Wojtowicz, Yong-Jie Wang, Xiaoguang Wu, and F. M. Peeters, Phys. Status Solidi B **229**, 597 (2002).
[3] Y. Imanaka, T. Takamasu, G. Kido, G. Karczewski, T. Wojtowicz, and J. Kossut, Physica B **256-258**, 457 (1998).
[4] M. Godlewski, W. M. Chen, and B. Monemar, Crit. Rev. Solid State Mater. Sci. **19**, 241 (1994).
[5] R. Romestain and C. Weisbuch, Phys. Rev. Lett. **45**, 2067 (1980).
[6] A. Moll, C. Wetzel, B. K. Meyer, P. Omling, and F. Scholz, Phys. Rev. B **45**, 1504 (1992).
[7] J. G. Michels, R. J. Warburton, R. J. Nicholas, and C. R. Stanley, Semicond. Sci. Technol. **9**, 198 (1994).
[8] W. M. Chen, N. T. Son, E. Janzen, D. M. Hofmann, and B. K. Meyer, Phys. Status Solidi A **162**, 79 (1997).
[9] S. I. Gubarev, A. A. Dremin, I. V. Kukushkin, A. V. Malyavkin, M. G. Tyazhlov, and K. von Klitzing, Pis'ma Zh. Eksp. Teor. Fiz. **54**, 361 (1991) [JETP Lett. **54**, 355 (1991)].
[10] N. Ahmed, I. R. Agool, M. G. Wright, K. Mitchell, A. Koohian, S. J. A. Adams, C. R. Pidgeon, P. C. Cavenett, C. R. Stanley, and A. H. Kean, Semicond. Sci. Technol. **7**, 357 (1992).
[11] R. J. Warburton, J. G. Michels, R. J. Nicholas, J. J. Harris, and C. T. Foxon, Phys. Rev. B **46**, 13394 (1992).
[12] H. A. Nickel, G. Kioseoglou, T. Yeo, H. D. Cheong, A. Petrou, B. D. McCombe, D. Broido, K. K. Bajaj, and R. A. Lewis, Phys. Rev. B **62**, 2773 (2000).
[13] H. A. Nickel, T. M. Yeo, A. B. Dzyubenko, B. D. McCombe, A. Petrou, A. Yu. Sivachenko, W. Schaff, and V. Umansky, Phys. Rev. Lett. **88**, 056801 (2002).
[14] C. J. Meining, H. A. Nickel, A. B. Dzyubenko, A. Petrou, M. Furis, D. R. Yakovlev, and B. D. McCombe, Solid State Commun. **127**, 821 (2003).
[15] A. Waag, S. Schmeusser, R. N. Bicknell-Tassius, D. R. Yakovlev, W. Ossau, G. Landwehr, and I. N. Uraltsev, Appl. Phys. Lett. **59**, 2995 (1991).
[16] E. L. Ivchenko, A. V. Kavokin, V. P. Kochereshko, G. R. Posina, I. N. Uraltsev, D. R. Yakovlev, R. N. Bicknell-Tassius, A. Waag, and G. Landwehr, Phys. Rev. B **46**, 7713 (1992).
[17] D. R. Yakovlev, W. Ossau, A. Waag, G. Landwehr, and E. L. Ivchenko, Phys. Rev. B **52**, 5773 (1995).
[18] C. R. L. P. N. Jeukens, P. C. M. Christianen, J. C. Maan, D. R. Yakovlev, W. Ossau, V. P. Kochereshko, T. Wojtowicz, G. Karczewski, and J. Kossut, Phys. Rev. B **66**, 235318 (2002).
[19] G. V. Astakhov, D. R. Yakovlev, V. P. Kochereshko, W. Ossau, W. Faschinger, J. Puls, F. Henneberger, S. A. Crooker, Q. McCulloch, D. Wolverson, N. A. Gippius, and A. Waag, Phys. Rev. B **65**, 165335 (2002).
[20] C. Y. Hu, W. Ossau, D. R. Yakovlev, G. Landwehr, T. Wojtowicz, G. Karczewski, and J. Kossut, Phys. Rev. B **58**, R1766 (1998).
[21] *Physics of Group IV Elements and III-V Compounds*, Landolt-Börnstein, New Series, Vol. 17a, edited by O. Madelung, M. Schmitz, and H. Weiss (Springer-Verlag, Berlin, 1982).
[22] K. K. Kanazawa and F. C. Brown, Phys. Rev. **135**, A1757 (1964).
[23] A. L. Mears and R. A. Stradling, Solid State Commun. **7**, 1267 (1967).
[24] J. Waldman, D. M. Larsen, P. E. Tannenwald, C. C. Bradley, D. R. Cohn, and B. Lax, Phys. Rev. Lett. **23**, 1033 (1969).
[25] D. R. Cohn, D. M. Larsen, and B. Lax, Phys. Rev. B **6**, 1367 (1972).
[26] M. Grynberg, S. Huant, G. Martinez, J. Kossut, T. Wojtowicz, G. Karczewski, J. M. Shi, F. M. Peeters, and J. T. Devreese, Phys. Rev. B **54**, 1467 (1996).
[27] M. Cardona, N. E. Christensen, and G. Fasol, Phys. Rev. B **38**, 1806 (1988).
[28] M. Willatzen, M. Cardona, and N. E. Christensen, Phys. Rev. B **51**, 17992 (1995).
[29] A. A. Sirenko, T. Ruf, M. Cardona, D. R. Yakovlev, W. Ossau, A. Waag, and G. Landwehr, Phys. Rev. B **56**, 2114 (1997).
[30] D. L. Smith and C. Mailhiot, Rev. Mod. Phys. **62**, 173 (1990).
[31] U. Ekenberg, Phys. Rev. B **40**, 7714 (1989).
[32] S. Y. Savrasov, Phys. Rev. B **54**, 16470 (1996).
[33] R. J. Nicholas, S. Sasaki, N. Miura, F. M. Peeters, J. M. Shi, G. Q. Hai, J. T. Devreese, M. J. Lawless, D. E. Ashenford, and B. Lunn, Phys. Rev. B **50**, 7596 (1994).